IEEE Access
Multidisciplinary | Rapid Review | Open Access Journal

Received May 20, 2021, accepted June 7, 2021, date of publication June 11, 2021, date of current version June 18, 2021.

Digital Object Identifier 10.1109/ACCESS.2021.3088462

A Differential Light Intensity-Modulation Optical Fiber Bundles Designed for Milling Tool Vibration Measurement

BINGHUI JIA AND JING YU
School of Mechanical Engineering, Nanjing Institute of Technology, Nanjing 211167, China
Corresponding author: Binghui Jia (bhjia@njit.edu.cn)

This work was supported by the Innovation Fund of Nanjing Institute of Technology under Grant CKJA201801.

ABSTRACT Tool vibration occurs widely in various machining operations and is one of the main factors affecting machining quality and stability. Light intensity-modulation optical fiber displacement sensor has distinctive advantages and greatly potential in tool vibration measurement. In order to overcome the shortages of conventional reflective light intensity modulation fiber bundle in small measurement range or low sensitivity, a novel differential light-intensity optical fiber bundles were proposed for measuring the high-speed milling tool vibration displacement. The mathematical model was demonstrated based on differential light-intensity modulation principle for sensing characteristics analyzing in this paper, firstly; then, the static calibration platform and the dynamic experiment platform were established to verify the differential light intensity-modulation characteristic of the fiber bundles; in the end, the static calibration experiment results shown that the measurement range of the differential light-intensity fiber bundles is more than 2mm, which expanded the measurement range of conventional fiber bundle by two times while improving the sensitivity obviously. The dynamic experimental results confirm the operating principle of differential light-intensity optical fiber bundles well. It has greatly availability applied for on-line precision measurement of tool vibration in milling machines.

INDEX TERMS Milling tool vibration, vibration measurement, optical fiber sensors.

I. INTRODUCTION

CNC milling machine plays an irreplaceable role in processing and manufacturing. Tool vibration occurs widely in various machining operations and is one of the main factors affecting machining quality and stability. Forced vibration is the main factor of tool vibration, resulting in the reduction of machining accuracy and efficiency, wear or life attenuation of the tool rapidly. It not only brings poor surface quality of parts, but also even causes rapid development of flutter failure or milling system collapse. Therefore, the measurement, prediction and suppression of tool vibration are always the research difficulty and hot spots [1], [2], and attracting more and more scholars and engineers' attention and research [3]–[5]. Because the vibration signal obtained directly determines the results of tool condition monitoring, fault diagnosis and performance evaluation, on-line tool vibration measurement technology have long been a key problem in high-speed milling. Although existing sensors have been widely used in tool vibration signal detection, there are many problems facing. For example, Lu [6] developed a micro-milling vibration measurement system based on laser displacement sensor. Tsai *et al.* [7] proposed a real-time flutter detection method based on acoustic emission, and then applied the acoustic feedback signal to the speed control of spindle motor. Huang *et al.* [8] used force and acceleration sensors to identify the milling chatter, and sort out the contribution of force on milling chatter at different frequencies. Lamraoui *et al.* [9] proposed a methodology for chatter detection in computer numerical control milling machines based on motor current signal monitoring. In practice, the laser displacement sensor needs to be specially designed and installed far away from the tool system in milling vibration measurement [10]; The microphone does not have strong anti-interference ability, and it is very sensitive to the noise in machining. When the microphone is used, apart from the direction of microphone layout needs to be considered, how to remove the mixed noise is a difficult problem be solved [11]; the application

The associate editor coordinating the review of this manuscript and approving it for publication was Ravibabu Mulaveesala.

of force sensor is greatly limited because of the shortcomings of high price, poor economy, not easy to install and low flexibility. Although the current sensor has the advantage of easy to install and flexible, but have low sensitivity and anti-interference ability, which not suit for early harmful vibration signals acquiring that hidden in noise [12]. Compared with the sensors mentioned above, optical fiber sensors offer distinctive advantages in that they are usually small size, light weight, high measurement accuracy, corrosion resistance, high temperature resistance, strong resistance to electromagnetic interference and atomic radiation, and easy to miniaturize design. They have significant advantages applying for parameter measurement in cutting process [13], [14]. Among them, the reflected light intensity modulation optical-fiber displacement sensors have simple structure, small size, ease integration, electromagnetic interference resistance, corrosion resistance and high detection sensitivity, those advantages make it especially suiting for the precision vibration displacement measurement of high-speed motion target [15]–[18], and be conductive to early unstable tool vibration information acquisition and recognition. Nevertheless, the measurement range and sensitivity of conventional reflective light intensity modulation fiber bundle should be improved when it is applied to milling tool vibration measurement.

In this paper, based on the principle of conventional reflective light intensity optical fiber displacement sensor, a differential light intensity modulation fiber bundles were put forward for the precision measurement of high-speed milling tool vibration. There are mainly two parts of the paper: The model of differential light intensity optical fiber bundles used for milling tool vibration and the measurement performance verification of the fiber bundles. The previous part will give the model of differential light intensity modulation fiber bundles and its design parameters; and the second part are the experiment results of the static calibration measurement, dynamic measurement and the milling tool vibration measurement of the fiber bundles. The proposed measurement method offers the advantages of

① reduces the effects of temperature change, power supply fluctuation and machine tool vibration on the measurement accuracy of the sensor effectively, avoids the common mode error and reduces the sensor nonlinear error,

② no interferences of electromagnetic noise,

③ in situ, direct measurements at fast rotating milling tool bar, which enables flexible integrations and allocabilities inside of machines cooling tube.

II. THE MODEL OF DIFFERENTIAL LIGHT-INTENSIGY OPTICAL FIBER BUNDLES

A. CONVENTIONAL LIGHT INTENSITY MODULATION PRINCIPLE OF FIBER BUNDLE

Fig.1 shows the working principle of conventional reflective intensity-modulated optical fiber displacement bundle. The fiber bundle consists of two parts: the emitting fiber (EF)

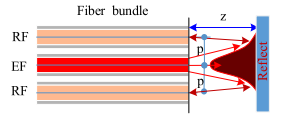

FIGURE 1. Conventional structure of reflective light intensity modulation optical fiber bundle.

and the receiving fiber (RF). Several receiving fibers always designed symmetric arrangement center about the emitting fiber in order to receive more light in application [19]. The distance between the EF and the RF is p, and the gap between the reflector and the probe is z. When the fiber bundle working, light emits from the EF in a conical shape (actually approximate a Gaussian distribution) and launch to the object surface, then the light reflected by the object surface, some or all light is received by the RFs. When the gap(z) changed, the reflected light intensity from the reflector is modulated. It means that the receiving light intensity of RFs change according with the displacement between the RF and reflector. At last, the light signal received by RF is converted to electrical signals by photodetector. In fact, the light intensity received by the RFs effecting by the gap between the reflector and the probe, the distance (p) RF to EF, the numerical aperture (NA) and the radius of RF&EF respectively. Usually, when the structural parameters of the fiber bundle were designed, the light intensity received by the RFs modulated by the gap between reflector and the fiber probe only.

The typically reflect light intensity-modulated character curve is shown as figure 2. It can be seen that there are two selectable measurement line ranges of the cure, the front slope with high sensitivity but small measurement range, the back slope with low sensitivity but larger measurement range compared with the front slope, it is not desirable in practical application.

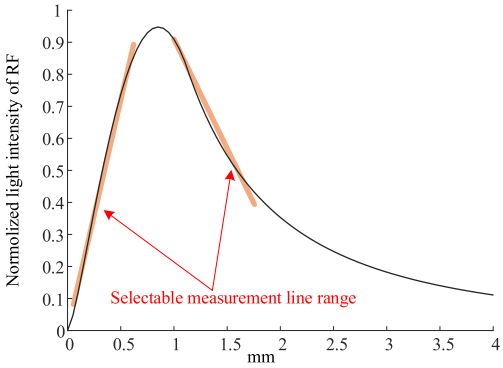

FIGURE 2. Conventional reflect light intensity-modulated character curve of RF.

B. DIFFERENTIAL LIGHT INTENSITY MODULATION PRINCIPLE OF FIBER BUNDLES

Focus above shortcoming, the differential light-modulation optical fiber displacement bundles for tool vibration

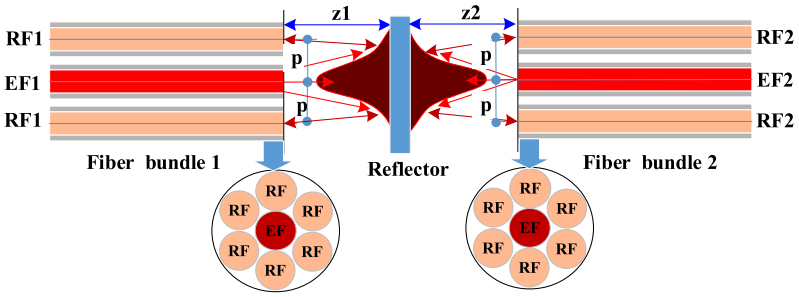

FIGURE 3. Differential modulation optical fiber displacement bundles.

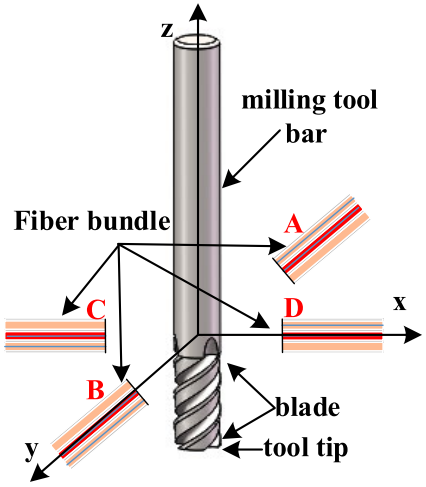

(a) fiber bundles position relative to the tool

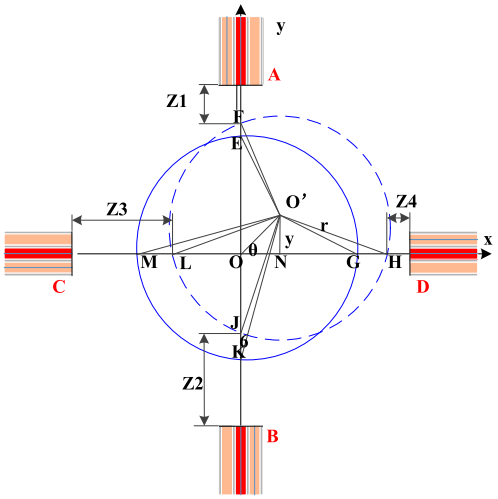

(b)Model of fiber bundles for tool vibration measurement

FIGURE 4. Model of multi-fiber bundles for milling tool vibration.

measurement was proposed. The differential light intensity modulation principle diagram is shown as figure 3. Different with conventional reflective light intensity modulation optical fiber displacement bundle shown in figure 1, there are two fiber bundles distribution on both sides of the reflector symmetrically. The light emits from EF1 and EF2 and launch to the two sides of reflector respectively, then the light reflected by each side of the object surface, some or all light received by the RF1 and RF2. As figure 3 shown, when the reflector move to left, the gap(z1) between fiber bundle1 probe and the reflector is reduced, meanwhile, the gap(z2) between fiber bundle2 probe to the reflector is increased. The movement of the reflect is modulated by the reflective light intensity of fiber bundles1 and fiber bundle2 at the same time; what's more, the light received by RF1 and RF2 are closely connected. The differential modulation optical fiber bundles structure have higher sensitivity to the reflector movement obviously.

Based on the differential light intensity modulation principle of fiber bundles, consider the tool surface shape, the mathematical model of multi-fiber bundles for milling tool vibration is established in figure 4.

To simplify the analysis, the radius and numerical aperture of the fiber bundles are equally designed, and four fiber bundles with the same structure parameters (six RFs surround the middle EF) are arranged around the tool as figure 3 shown, the rectangular coordinate system is established. The initial center of the tool 'O' is denoted as the coordinate system origin, and the tool center is marked as $O'(x, y)$ after vibration at a particular point in time. The distances between fiber bundle A and the tool surface, the distances between fiber bundle B and the tool surface in y direction are denote as Z1, Z2 respectively; the distances between fiber bundled C and the tool surface, the distances between fiber bundle D and the tool surface in x direction are denote as Z3, Z4 respectively. Assuming that the tool radius is R, and the original distance of four fiber bundles to tool surface are q, the distances of fiber bundle A, fiber bundle B, fiber bundle C and fiber bundle D to the tool surface are Z_1, Z_2, Z_3, Z_4 as figure 4 shown.

For fiber bundle A: In the triangle $OO'F$, have:

$$\frac{OO'}{sin\angle OFO'} = \frac{O'F}{sin\angle FOO'} = \frac{OF}{sin\angle OO'F} \tag{1}$$

$$\theta = arctan(\frac{y}{x}) \tag{2}$$

$$OF = \frac{OO' \cdot sin\angle OO'F}{sin\angle OFO'} \tag{3}$$

$$Z_1 = R + q - OF = R + q - \frac{Rsin(\frac{\pi}{2} - \theta + arcsin\frac{\sqrt{x^2+y^2}\cdot cos\theta}{R})}{cos\theta} \tag{4}$$

For fiber bundle B: In the triangle *OO'J* have:

$$\frac{OO'}{sin\angle OJO'} = \frac{O'J}{sin\angle JOO'} = \frac{OJ}{sin\angle OO'J} \tag{5}$$

$$OJ = \frac{OO' \cdot sin\angle OO'J}{sin\angle OJO'} \tag{6}$$

$$Z_2 = R + q - OJ = R + q - \frac{Rsin(\frac{\pi}{2} + \theta + arcsin\frac{\sqrt{x^2+y^2}\cdot cos\theta}{R})}{cos\theta} \tag{7}$$

For fiber bundle C: In the triangle *O'LN*, have:

$$LN = \sqrt{LO'^2 - O'N^2} = \sqrt{R^2 - y^2} \tag{8}$$

$$LO = LN - ON = LN - x \tag{9}$$

$$Z_3 = R + q + x - \sqrt{R^2 - y^2} \tag{10}$$

For fiber bundle D: In the triangle *O'LN*, have:

$$NH = \sqrt{HO'^2 - O'N^2} = \sqrt{R^2 - y^2} \tag{11}$$

$$HO = HN + ON = HN + x \tag{12}$$

$$Z_4 = R + q - x - \sqrt{R^2 - y^2} \tag{13}$$

According to the mode theory of optical fiber transmission, as many scholars did, the radial distribution of the combined light intensity in the optical output field can be approximated by the Gaussian function [19], [18], and the received light intensity of fiber bundle A, fiber bundle B, fiber bundle C and fiber bundle D can be calculated by equation (14).

$$I = \frac{\rho \iint_{S_r} K_0\varphi(r,z)\cdot exp[-\eta r]dS_r}{\rho \iint_{S_t} K_0\varphi(r,z)\cdot exp[-\eta r]dS_t} + I_{\text{noise}} \tag{14}$$

where $\varphi(r, z)$ is the light flux density of the position (rz), can be written as equation(15).

$$\varphi(r,z) = \frac{I_0}{\pi\omega(z)} exp\left[-\frac{r^2}{\omega(z)^2}\right] \tag{15}$$

K_0 is the loss of light in emitting fiber $exp[-\eta r]$ is the additional loss of optical intensity due to fiber bending; S_r is the effective receiving area of the RF; S_t is the facula area reflected from the reflector; I_{noise} denote as the noise because of the reflective surface shape and environment changes. ρ is the associated parameter which indicates the distribution of fiber refractive index. I_0 is the light strength that light source coupled in the fiber. $\omega(z)$ is the equivalent radius of optical field distribution, and:

$$\omega(z) = a_0\left[1 + \xi\left(\frac{z}{a_0}\right)tan(\theta_0)\right] \tag{16}$$

In equation (16), a_0 is the fiber radius; ξ is the modulation parameter related to the fiber coupling conditions; θ_0 is the maximum fiber emergence angle.

Based on equation (14), consider the tool surface is convex, the facula area reflected from the reflector is elliptical shape, denote as the transverse a and the minor axis b; the expression of receiving light intensity of RF in cartesian coordinate system can be written as, (17) and (18), as shown at the bottom of the page,

where S_{r1}, S_{r2}, S_{r3} and S_{r4} are the effective receiving area of the RFs of fiber bundle A, B, fiber C and D, respectively. πa_1b_1, πa_2b_2, πa_3b_3 and πa_4b_4 are facula area reflected from tool to the fiber bundles A, B, C and D, which determined by the reflector surface shape, the NA of EF and the distances fiber probes to tool surface. Assume that the small angle change of the reflective surface changes due to tool vibration is α, based on the geometric positional relationships shown in figure 3(b), S_{r1},S_{r2}, S_{r3} and S_{r4} can be gained:

$$S_{r1} = 2\left(\int_{p-r}^{\frac{2z_1}{cot(\theta_0-\alpha)+tan\alpha}+r-a_1}\sqrt{r^2-(x-p)^2}dy + \int_{\frac{2z_1}{cot(\theta_0-\alpha)+tan\alpha}+r-a_1}^{a_1+\frac{2z_1}{cot(\theta_0-\alpha)+tan\alpha}+r-a_1}\sqrt{b_1^2\left(1-\frac{(x-\frac{2z_1}{cot(\theta_0-\alpha)+tan\alpha}+r-a_1)^2}{a_1^2}\right)}dy\right) \tag{19}$$

$$S_{r2} = 2\left(\int_{p-r}^{\frac{2z_2}{cot(\theta_0-\alpha)+tan\alpha}+r-a_2}\sqrt{r^2-(x-p)^2}dy + \int_{\frac{2z_2}{cot(\theta_0-\alpha)+tan\alpha}+r-a_2}^{a_2+\frac{2z_2}{cot(\theta_0-\alpha)+tan\alpha}+r-a_2}\sqrt{b_2^2\left(1-\frac{(x-\frac{2z_2}{cot(\theta_0-\alpha)+tan\alpha}+r-a_2)^2}{a_2^2}\right)}dy\right) \tag{20}$$

$$S_{r3} = 2\left(\int_{p-r}^{\frac{2z_3}{cot(\theta_0-\alpha)+tan\alpha}+r-a_3}\sqrt{r^2-(x-p)^2}dx\right.$$

$$I_{A-B} = n\cdot\left(\frac{S_{r1}\cdot\rho\iint_{S_{r1}}K_0\varphi(r,z_1)\cdot exp[-\eta r]dS_{r1}}{\pi a_1b_1} - \frac{S_{r2}\cdot\rho\iint_{S_{r2}}K_0\varphi(r,z_2)\cdot exp[-\eta r]dS_{r2}}{\pi a_2b_2}\right) \tag{17}$$

$$I_{D-C} = n\cdot\left(\frac{S_{r4}\cdot\rho\iint_{S_{r1}}K_0\varphi(r,z_4)\cdot exp[-\eta r]dS_{r4}}{\pi a_4b_4} - \frac{S_{r3}\cdot\rho\iint_{S_{r2}}K_0\varphi(r,z_3)\cdot exp[-\eta r]dS_{r3}}{\pi a_3b_3}\right) \tag{18}$$

$$+\int_{\frac{2z_3}{cot(\theta_0-\alpha)+tan\alpha}+r-a_3}^{a_3+\frac{2z_3}{cot(\theta_0-\alpha)+tan\alpha}+r-a_3} \times\sqrt{b_3^2(1-\frac{(x-\frac{2z_3}{cot(\theta_0-\alpha)+tan\alpha}+r-a_3)^2}{a_3^2}}dx) \quad (21)$$

$$S_{r4}=2(\int_{p-r}^{\frac{2z_4}{cot(\theta_0-\alpha)+tan\alpha}+r-a_4}\sqrt{r^2-(x-p)^2}dx +\int_{\frac{2z_4}{cot(\theta_0-\alpha)+tan\alpha}+r-a_4}^{a_4+\frac{2z_4}{cot(\theta_0-\alpha)+tan\alpha}+r-a_4} \times\sqrt{b_4^2(1-\frac{(x-\frac{2z_4}{cot(\theta_0-\alpha)+tan\alpha}+r-a_4)^2}{a_4^2}}dx) \quad (22)$$

Substitute the equation (4), (7) into equation (17), and (10), (13) into equation (18), have:

Based on equation (23) and (24), as shown at the bottom of the page, the light strength of the differential intensity optical fiber bundles in the X and Y directions can be gained, which mean the vibration displacement of tool in the X and Y directions is measured.

C. SIMULATION OF THE FIBER BUNDLE MEASUREMENT FEATURE

As the optical fiber bundles in X and Y direction have similar structure, only the fiber bundles in y direction were analysis here. Based on equation (15), (16), (23) and (24) can be seen that the received light intensity of RF depends on the fiber radius and NA of RF and the EF, the distance between the RF and the EF, the vibration displacement of tool. In this paper, without considering the additional bending loss, and noting that $\xi = 0.5$, as many papers did [16]–[18], the fiber bundles are tightly arranged; in order to reduce the difficulty of fiber beam manufacturing, the same radius and numerical aperture of EF and RF were chosen, the normalized characteristic of I_y was simulated by changing one of the parameters each time.

1) EFFECT OF FIBER RADIUS ON THE OUTPUT CHARACTER OF I_y

The fiber radius of the EF and RFs were set as 100μm, 150μm,200μm,250μm,300μm respectively, where the NA is 0.22. The normalized characteristic curve of I_y is shown as figure 5. It can be seen that with the increase of the fiber

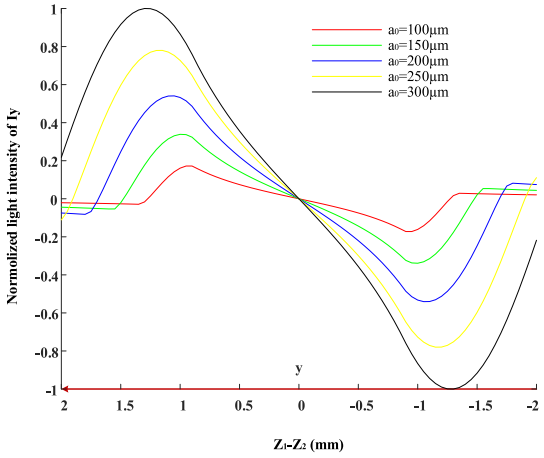

FIGURE 5. Normalized characteristic curve of I_y when fiber radius a0changes calculated by equation (24). (a_0 is 100μm, 150μm,200μm,250μm,300μm).

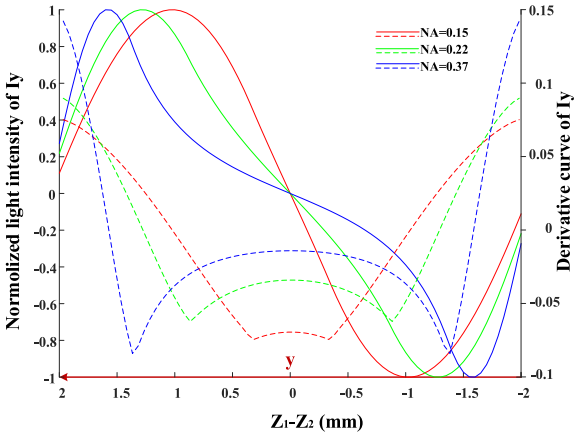

FIGURE 6. Normalized characteristic and derivative curves of Iy when NA changes (NA is 0.15, 0.22 and 0.37).

radius, the measurement range and sensitivity increase as well. It means that fiber bundle with bigger fiber radius have better measurement characteristic.

2) EFFECT OF THE NA ON THE OUTPUT CHARACTER OF I_y

The NA of the EF and RFs were set as 0.15, 0.22 and 0.37respectively, and withing fiber radius of 300μm. The normalized characteristic curve of I_y is shown in the left side of figure 6. It can be seen that fiber bundles with bigger NA have lager measurement range and higher sensitivity. But the

$$I_x = I_{D-C} = 6\cdot\left(\frac{S_{r1}\cdot\rho\iint_{S\,r1}K_0\varphi(r,R+q-\frac{Rsin(\frac{\pi}{2}-\theta+arcsin\frac{\sqrt{x^2+y^2}\cdot\cos\theta}{R})}{cos\theta})\cdot exp[-\eta r]dS_{r1}}{\pi a_1 b_1} - \frac{S_{r2}\cdot\rho\iint_{S\,r2}K_0\varphi(r,R+q-\frac{Rsin(\frac{\pi}{2}+\theta+arcsin\frac{\sqrt{x^2+y^2}\cdot cos\theta}{R})}{cos\theta})\cdot exp[-\eta r]dS_{r2}}{\pi a_2 b_2}\right) \quad (23)$$

$$I_y = I_{A-B} = 6\cdot\left(\frac{S_{r4}\cdot\rho\iint_{S\,r4}K_0\varphi(r,R+q+x-\sqrt{R^2-y^2})\cdot exp[-\eta r]dS_{r4}}{\pi a_4 b_4} - \frac{S_{r3}\cdot\rho\iint_{S\,r3}K_0\varphi(r,R+q-x-\sqrt{R^2-y^2})\cdot exp[-\eta r]dS_{r3}}{\pi a_3 b_3}\right) \quad (24)$$

curve of I_y with larger NA has obvious linearity error, which is shown as the right side of figure 6. This is mainly because the optical fiber with larger NA has stronger light receiving ability but interfered by other light easier.

3) THE NORMALIZED INTENSITY CHARACTERISTIC OF THE DIFFERENTIAL LIGHT INTENSITY-MODULATION FIBER BUNDLES

Therefore, consider the simulation results above and the tool vibration requirements comprehensively, the design parameters of differential light intensity-modulation fiber bundles were determined: the fiber radius of EF and RFs are 250μm, the NA is 0.22, and the single fiber bundle structure is shown as figure 7. The normalized intensity curve of the differential light intensity-modulation fiber bundles is shown in figure 8. It can be seen that compared with conventional reflective light intensity modulation optical fiber bundle as figure 2 showed, the measurement range and sensitivity of differential light intensity-modulation fiber bundles is greatly expanded.

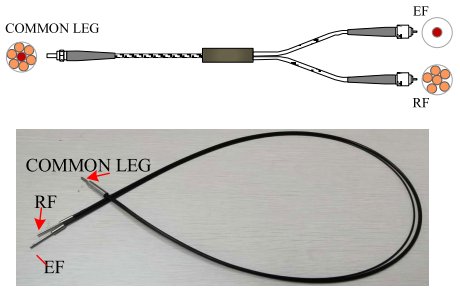

FIGURE 7. Structure of single fiber bundle and actual photograph.

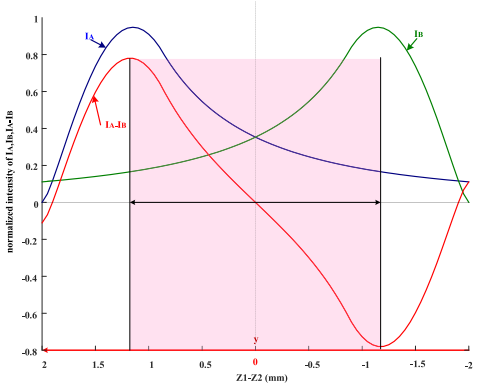

FIGURE 8. Normalized intensity curve of the differential light intensity-modulation fiber bundles.

In order to verify the characteristic of the differential light intensity-modulation fiber bundles we designed in this paper. The tool axis was assumed moving along a trajectory as figure 9 shown. The trajectory is controlled by equation (25), and the max vibration is 1mm of the tool.

$$\begin{cases} x = 0.05 \cdot \theta \cdot cos(\theta) \\ y = 0.05 \cdot \theta \cdot sin(\theta) \end{cases} \tag{25}$$

The tool vibration follows the trajectory in the XOY plane as figure 9 shown, and the normalized light intensity curve of the differential light intensity-modulation fiber bundles in x and y direction were shown in figure 10. It can be seen that when the tool moving from origin to fiber bundle B in the negative direction of y-axis in the third quadrant, the light intensity of I_y (I_A-I_B) drops rapidly; at the same time, when the tool moving from the origin to fiber bundle C first and then leave fiber bundle C to fiber bundle D in x-axis in the third quadrant, the light intensity of I_x (I_D-I_C) goes down slowly and then goes up. In the fourth quadrant, the I_y start to rise after holding on the variation trend in the third quadrant for a while, the light intensity of I_x keeps increasing all the time. In the first quadrant, I_y keeps increasing in the entire value range; however, because the tool near the fiber bundle D first and then away from it, which can be seen in figure 9 clearly, the light intensity of I_y gets a little bigger and then starts to get smaller quickly. In the second quadrant, both I_y and I_x reduce linearly approximately. The normalized intensity curve of the differential light intensity-modulation fiber bundles shown in figure 10 fitting the tool vibration trajectory accurately.

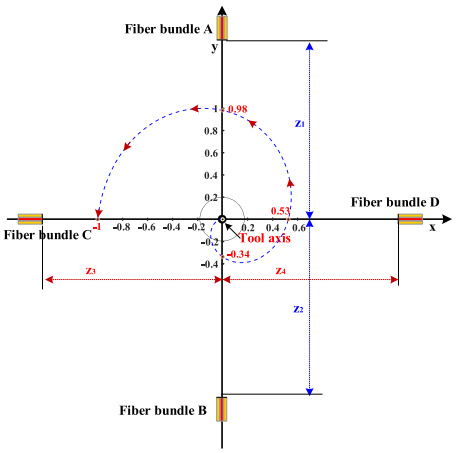

FIGURE 9. Tool axis moving trajectory in xoy plane.

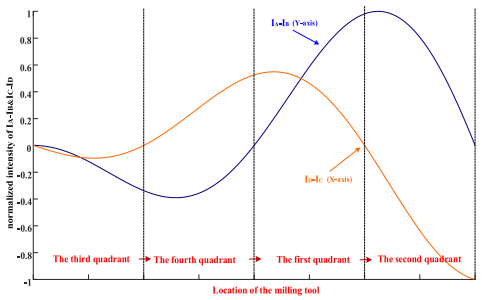

FIGURE 10. Normalized intensity curve of the differential light intensity-modulation fiber bundles.

III. EXPERIMENT RESULTS AND DISCUSSION

A. CONFIGURATION SYSTEM AND DYNAMIC TEST SETUP

The static calibration platform consists the moving platform in x direction and y direction respectively, a fixing bracket

of fiber bundle, and there are four mounting holes for fiber bundles; the tool is mounted on the top of the configuration platform, as figure 11 shown. The moving platform in x direction and y direction are driven by two micrometer crew gauge, which have a linear range of 10mm and the resolution of 0.01mm. When the calibration platform working, four fiber bundles designed as figure 7 shown are fixed in four mounting holes, and the tool is controlled moving in the z direction until the surface of tool bar facing to the fiber bundles probe. The distance between the tool and the fiber bundle probe can be adjusted by moving the position of the fiber bundle.

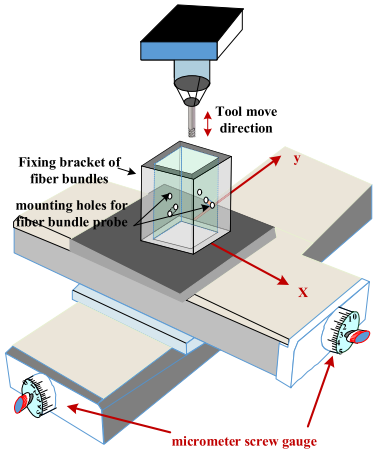

(a) Schematic diagram of static calibration platform

(b) photo of the calibration platform

FIGURE 11. Static Calibration Platform for fiber bundle.

The schematic diagram of dynamic test platform is shown as figure 12. It is beneficial to the coolant pipe on the machine, four fiber bundles in x and y direction were placed in these pipes, without changing the original machine structure. In this paper, a desktop milling machine was used for verifying the dynamic characteristic of the differential light intensity-modulation fiber bundles we designed. The milling machine was made by MENGCHAO Company, with the power of 480W, the speed adjustable range from 0 to 10000RPM, and the mountable milling tool diameter from 2mm to 8mm.

In experiment, the received light intensity of the RFs was converted to voltage signal by the OPT101 monolithic

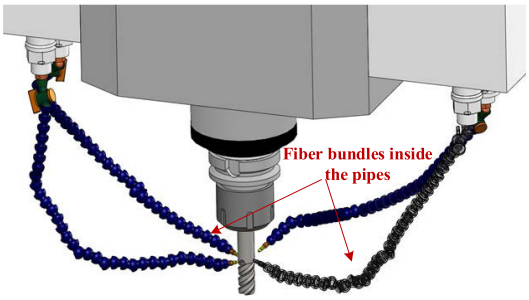

FIGURE 12. Schematic diagram of installation position of fiber bundle in machine tool.

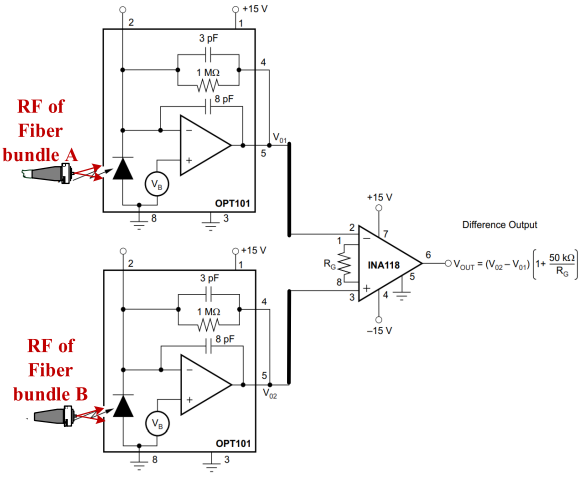

FIGURE 13. Differential light measurement in Y direction.

photodiode and single-supply transimpedance amplifier made by Texas Instruments Incorporated. And the 650nm red light source was chosen. The applications circuit that was used for differential light sensing of fiber bundle A and fiber bundle B in Y direction is shown as figure 13, the same with X direction. At last, a NI acquisition card was used to gain the signals and store to computer.

The maximum signal frequency of the sensor system designed by us is 50kHz. Taking the 4-edge milling tool as example, the maximum speed of the tool that can be measured by the system designed in this paper is 300,000 RPM, which is faster than the rotation speed of most machine tool spindles on the market.

B. RESULTS AND DISCUSSION

1) STATIC CALIBRATION RESULTS

In experiment process, a milling tool with diameter of 8mm was chosen, the initial distance between the probe and the tool is 2mm, and the forward direction of x-axis and y-axis were denoted as positive displacement, the backward direction of x-axis and y-axis were denoted as negative displacement. The knob of the micrometer crew gauge was adjusted to move in the range of $\pm 1000\mu$m in X direction with a step of 20μm, and keeping the micrometer crew gauge motionless in Y direction. The experiments were repeated 30 times and the data of each experiments were recorded, then the process

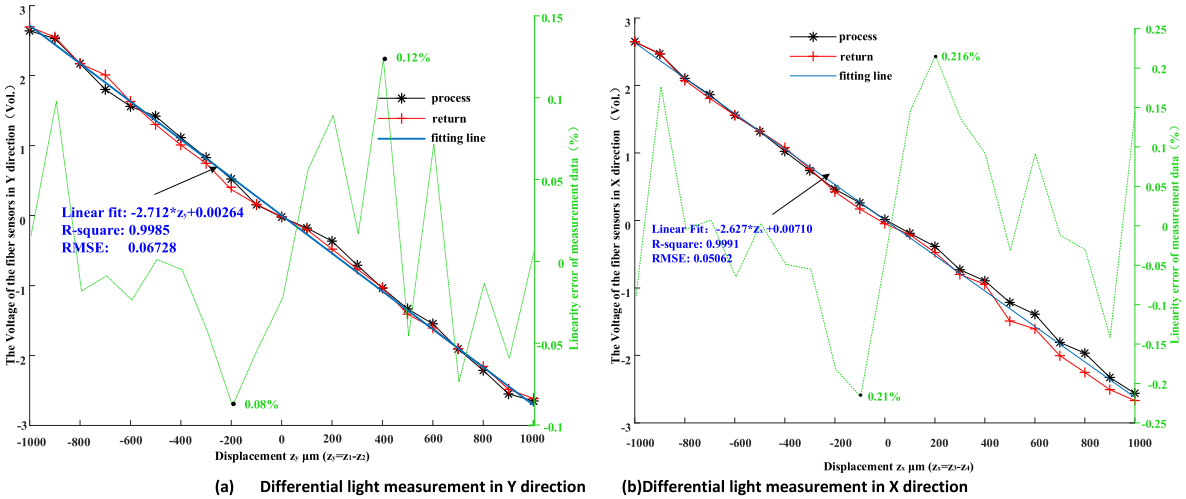

(a) Differential light measurement in Y direction (b)Differential light measurement in X direction

FIGURE 14. Differential light converted to voltage in X &Y direction.

data and return data was averaged respectively. Similar work was done in the X direction. And the fitting curve of the differential light measured in X & Y directions are shown as figure 14, which has been converted to a voltage signal.

a: LINEAR MEASUREMENT RANGE

It can be seen that the differential light intensity-modulation fiber bundles have very good linearity in the measurement range of 2mm in x direction and y direction. The sensitivity is 2.668mv/μm, and 2.623mv/μm of y direction and x direction respectively, as equation (26) and (27) shown.

$$S_y = \frac{\Delta V}{\Delta z} = \frac{[2.634 - (-2.702)]\,v}{2000\mu m} = \frac{5336mV}{2000\mu m} = 2.668mv/\mu m \tag{26}$$

$$S_x = \frac{\Delta V}{\Delta z} = \frac{[2.626 - (-2.620)]\,v}{2000\mu m} = \frac{5246mV}{2000\mu m} = 2.623mv/\mu m \tag{27}$$

b: ACCURACY AND PRECISION OF MEASUREMENT

As figure 14 shown, the linearity error of measurement data (the green curve) is calculated by the difference between the average of process and return data and the linear fit data dividing the measurement range. It can be seen that the maximum linear error in y direction is 0.12%, and the maximum linear error in x direction is 0.216%, which mean that the max measurement error in x direction is 4.32μm (the measurement range 2000μm multiply by the maximum linear error 0.216% equal to 4.32μm), max measurement error in y direction is 2.4μm (the measurement range 2000μm multiply by the maximum linear error 0.12% equal to 2.4μm). Combined with the above analysis, the accuracy and precision of the sensor is 0.216% in x direction, and the accuracy and precision of the sensor in y direction is 0.12%. And the reasons of why the maximum measurement error in X direction different with the Y direction mainly caused by the manufacturing error, installation deviation, photoelectric conversion efficiency difference of photoelectric conversion devices and so on. As four fiber bundles and their subsequent processing circuits are not identical, the differences in measurement errors are unavoidable.

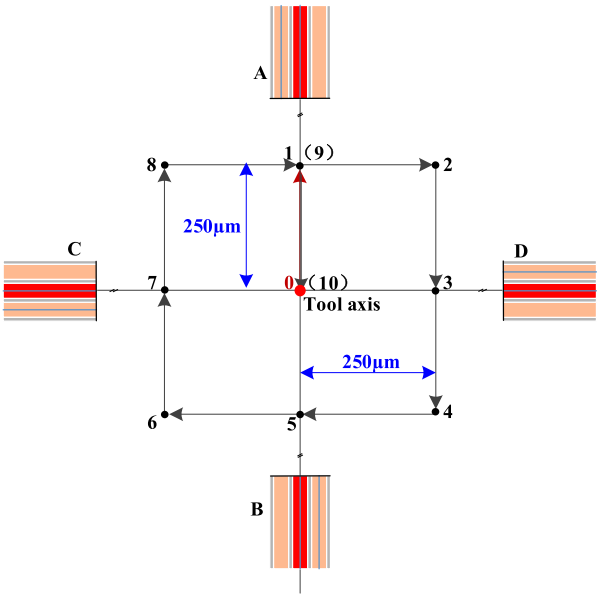

FIGURE 15. Square motion paths of the tool axis.

c: THE TRACKING OF TOOL TRAJECTORY

As a matter of fact, the vibration of the tool is a spatial concept, though, we measure the tool vibration displacement in x and y direction only, the movement of the tool happens in the XOY plane. To test the measurement characteristics of the fiber bundles when tool deviates from the positive direction of the axes, and considering the difficult task that controlling the tool axis moves accurately as the trajectory shown in figure 9 in xoy plane, a simplified square motion paths was designed as figure 15 shown. There are 10 part of the entire trajectory in figure 15, the length of each part

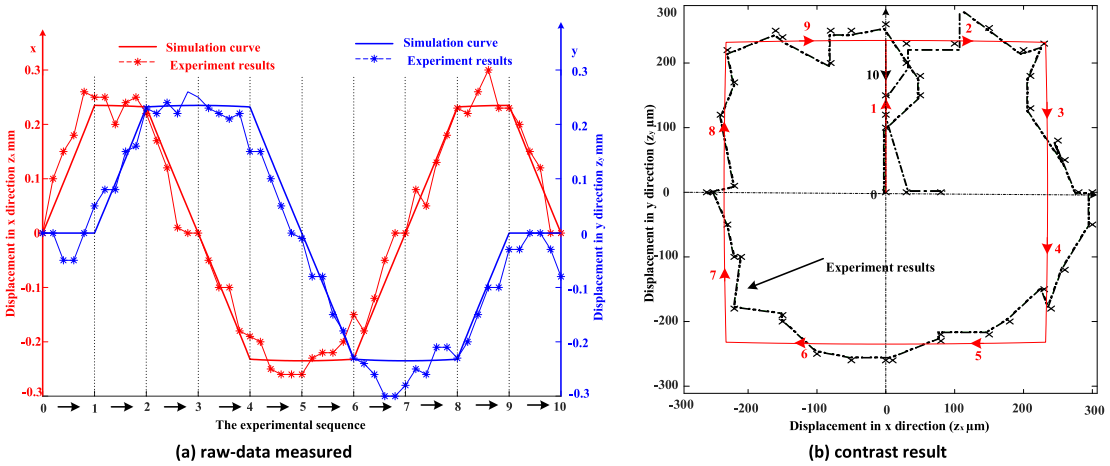

FIGURE 16. Measurements results of the fiber bundles under a given motion trajectory.

is 250μm. In experiment, the micrometer crew gauge was adjusted following the trajectory from the origin with a step of 50μm one time. The simulation curve and the experiment raw data is shown in figure 16(a), and the contrast result is shown in figure 16 (b). The blue line and the red line are simulation curves, and the blue star-shaped curve and the red star-shaped curve are the experiment results in y direction and x direction respectively in figure 16(a); the red line is the ideal trajectory of the tool axis, and the dotted black line with x is the actual track of the tool axis based on measurement in figure 16(b). It can be seen that the changing trend of the measurement curve fitting the simulation results very good. Because the moving direction of the micrometer crew gauge is very frequently, the motion errors of the plate was introduced to the measurement results inevitably, which caused the measurement results deviation from the satisfactory result. Comprehensive the static calibration experimental results in figure 14, the actual effect of the tracking results is good.

The fiber bundles were mounted in the pipes shown as figure 12, and the alligation milling tool diameter is 6mm. Keep machine not working, a transient force about 5N was exerted on the tool tip quickly in x direction by a PCB impact hammer. The tool vibration displacements in x and y direction caused by the impacting force were synchronal measured by the fiber bundles. The measurement results curves after filtering are shown in figure17. It can be seen that there is a transient vibration of the tool in x and y directions, and the transient variation tendency curves last about 0.05s and conform the impulse response characteristic of milling tool system very good. The max vibration displacement of the tool is 6.96μm in x direction, and the max vibration displacement is 2.69μm in y direction. Which mean the differential light intensity-modulation fiber bundles are very sensitive to the tool vibration signal. It can be used for tool vibration on line measurement.

As the fiber bundles designed focusing on dynamic tool vibration measurement, in order to verifying the dynamic measurement characteristics and the ability used for different

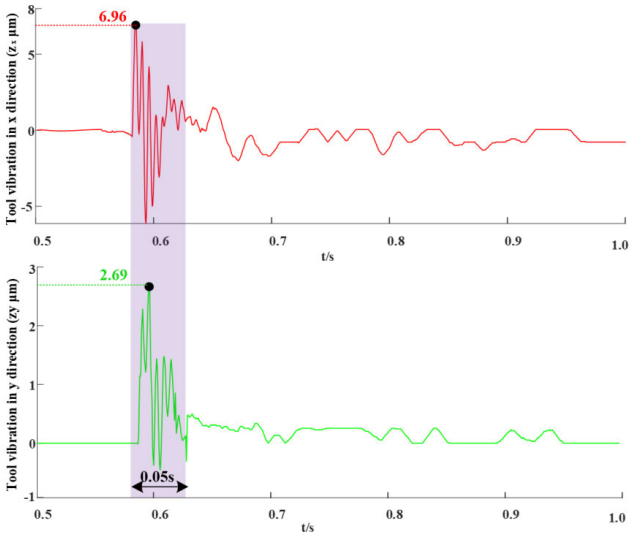

FIGURE 17. Impulse responses test of the differential light intensity-modulation fiber bundles.

diameter tools of the measurement system, the dynamic tool vibration measurement experiment was done and the measurement results of the tool vibration displacement in machine start-stop process are shown in figure18, the red line and the blue line are the tool vibration displacements in x and y direction respectively. In the experiment process, 3 milling tools with the diameter of 2mm, 6mm&8mm were used respectively. The machine tool spindle speed is controlled increase from 500 to 5000RPM in 1 seconds during startup, then keep the spindle speed for a moment (1 to 2 second), after that the spindle speed is controlled reduce from 5000 to 0 RPM in 1 seconds quickly, the whole start-stop process took 4 seconds. In figure 18, it can be seen that the machine has a similar vibration change curve during starting, constant speed and stopping. The vibrations amplitude increases rapidly during starting and stopping, and the vibration amplitude is smaller and remained relatively stable at the uniform speed. As figure 18 shown,

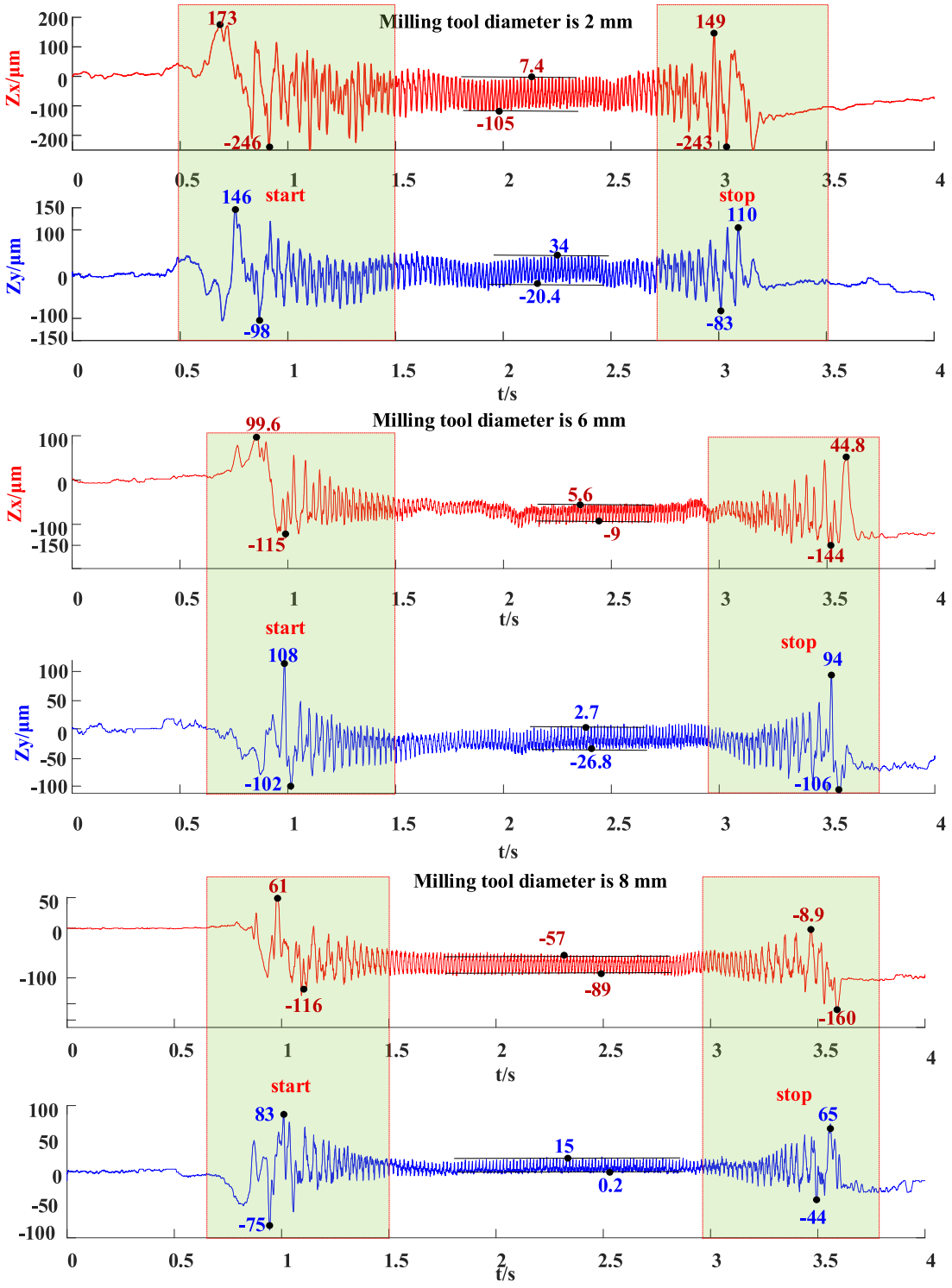

FIGURE 18. The tool vibration measurement experiment result in machine start-stop process.

the vibration ranges of the tools (diameter is 2 mm,6mm and 8mm, respectively) are 419μm, 214.6μm, 177μm in x direction, and the vibration ranges are 244μm, 210μm and 158μm in y direction in machine start process, respectively; the vibration ranges are 392μm, 188.8μm and 151μm in x direction, 193μm, 200μm, 110μm in y direction, respectively; the minimum vibration ranges of 3 tools are 54.4μm,14.6μm and 14.8μm when keep the machine operating with a constant speed of 5000RPM. It can be seen that t the vibration amplitude of the tool withing diameter of 2mm, 6mm and 8mm decrease orderly in start-stop process, which more obviously during starting and stopping process. It mainly because the tool withing smaller diameter has higher flexibility, when the spindle speed crosses the first natural frequency of the

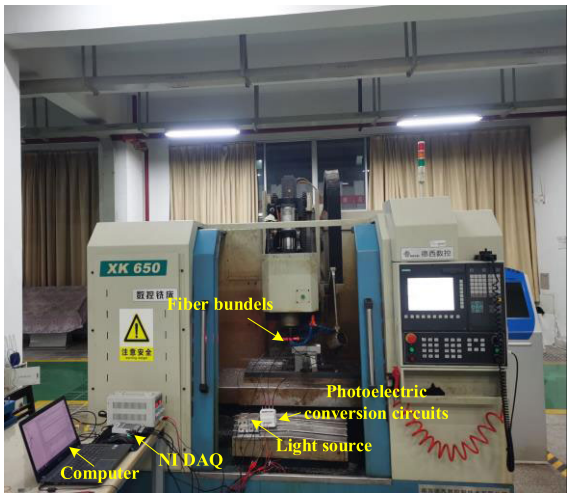

FIGURE 19. Experiment platform.

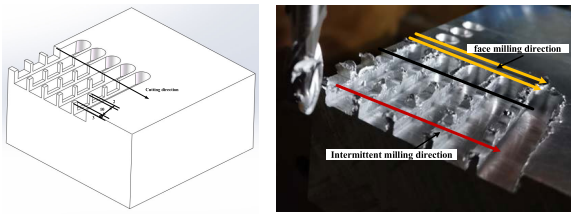

（a）3D map of the workpiece （b）Photos of workpiece

FIGURE 20. Intermittent milling of thin-walled structures.

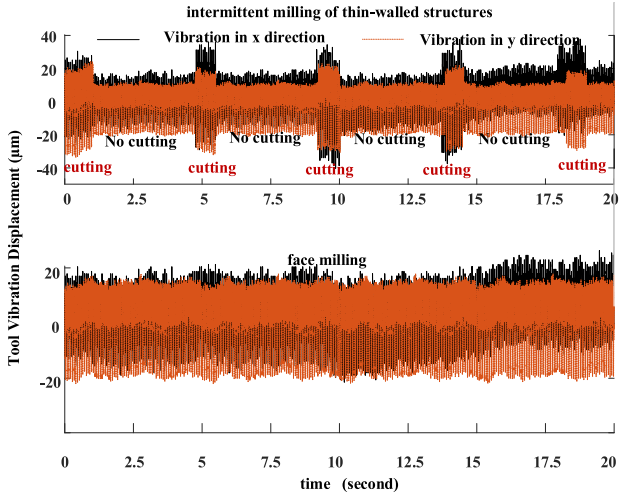

FIGURE 21. Intermittent milling of thin-walled structures (above curve) and face milling with the same cutting parameters (below curve) (a set of raw test data).

milling tool system, a stronger vibration is aroused, the curve in figure 18 confirmed this clearly. The accurate acquisition of these fine vibration signal changes also proves that the differential light intensity-modulation fiber bundles designed in this paper have good dynamic characteristics.

2) TOOL VIBRATION MEASUREMENT VERIFIES IN MILLING MACHINE ENVIRONMENTS

In order to verify the method proposed in this paper for tool vibration measurement that in complex milling machine

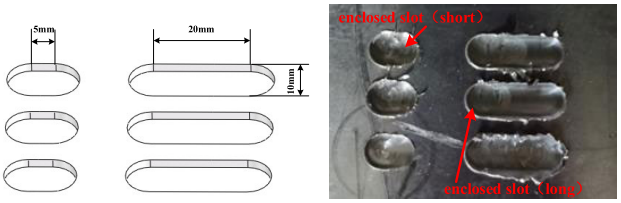

(a) Schematic diagram of the slot to be machined (b) the machined slots

FIGURE 22. Enclosed slots milling.

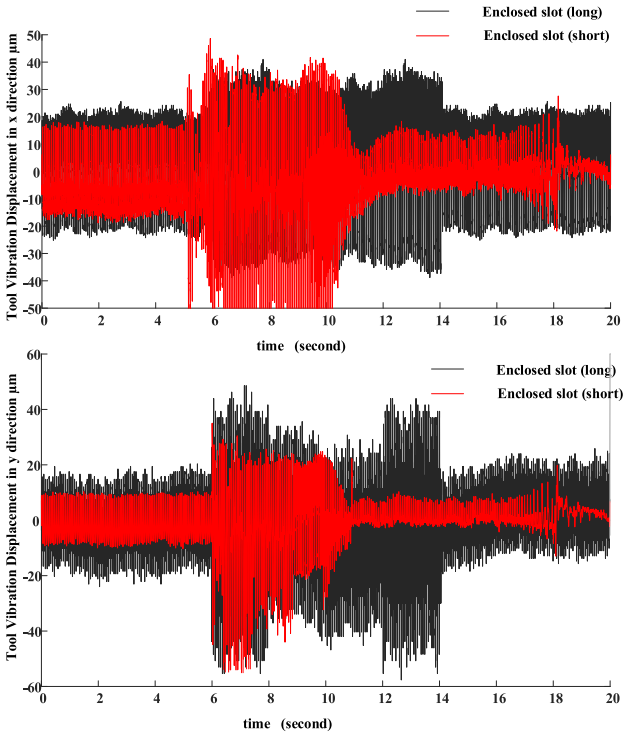

FIGURE 23. The tool vibration displacement when enclosed slots processing: the first line enclosed slots milling (above curve) and the third line enclosed slots milling (bellow curve) in figure 22.

environments. The experiment platform is shown as figure 19, the maximum RPM of the CNC is 8000, it can be used for board classes, plates, shell, precision parts machining. Part of the experiments results are shown in figure 20 to figure 23. Figure 20 shows the thin-walled structures after processing and figure 21 shows the tool vibration when intermittent milling of thin-walled structures process and face milling process, with the same speed of 3000RPM, cutting deep of 1.5mm, feed of 0.4/r. Compared with two courses of working, it can be seen that the tool vibration displacement signal in above processed mainly including of tool vibration and noise; however, the different of the tool vibration displacement signal in intermittent milling of thin-walled structures process is very clearly, it indicate that the method proposed in this paper have the ability of working in machine environment. Figure22 and figure 23 shown the tool vibration results of enclosed slots milling process. Compared with the tool vibration signals of short enclosed slot process and long enclosed slot process, it can be seen that little different tool vibration signal can be captured by the measurement system.

What's more, carefully observing the processed enclosed slots in the first row and the third row in Fig. 22, it can be found that the enclosed slot (short) in the first row is larger than the third row, while the long-enclosed slot in the first row is smoother than the long-enclosed slot in the third row. By comparing the measurement results shown in Fig. 23, it can be found that there is a significant difference between the vibration signal of the processing of the first row and the third row. those experiments proved the fiber bundles having the ability of working in milling machine environmental.

IV. CONCLUSION

A novel differential light-intensity optical fiber bundles used for high-speed milling tool vibration displacement measurement is proposed in this paper. The shortages of conventional reflective light intensity modulation fiber bundle without desirable measurement range and sensitivity are overcome in tool vibration. In order to verify the differential light intensity-modulation characteristic of the fiber bundles, a static calibration platform and the dynamic experiment platform were established. The static calibration experiment shows that the measurement range of the differential light intensity fiber bundles is more than 2mm, which expanded the measurement range of conventional fiber bundle by two times while improving the sensitivity obviously. The maximum linear error of the sensor is 0.216%. The dynamic tool vibration measurement results show that the fine tool vibration signal changes can be precisely obtained during machine start-stop process based on the differential light-intensity optical fiber bundles we designed. The experimental results not only confirm the operating principle of the differential light-intensity optical fiber bundles well, but also fully benefits the flexible characteristics of optical fiber materials, which can be mounted in the machine cooling pipe without changing the initial machine structure. Although the feasibility of the method is proved in application of tool vibration measurement by the results of theoretical analysis and experiment, there are still some problems that need to be further analyzed in future research, such as the reliability of the sensor, how to integrate the sensors into the machine tool and avoid the impact of installation errors.

REFERENCES

[1] L. Zhu and C. Liu, "Recent progress of chatter prediction, detection and suppression in milling," *Mech. Syst. Signal Process.*, vol. 143, Sep. 2020, Art. no. 106840.
[2] C. Yue, H. Gao, X. Liu, S. Y. Liang, and L. Wang, "A review of chatter vibration research in milling," *Chin. J. Aeronaut.*, vol. 32, no. 2, pp. 215–242, Feb. 2019.
[3] D. Li, H. Cao, and X. Chen, "Fuzzy control of milling chatter with piezoelectric actuators embedded to the tool holder," *Mech. Syst. Signal Process.*, vol. 148, Feb. 2021, Art. no. 107190.
[4] T. J. Gibbons, E. Ozturk, L. Xu, and N. D. Sims, "Chatter avoidance via structural modification of tool-holder geometry," *Int. J. Mach. Tools Manuf.*, vol. 150, Mar. 2020, Art. no. 103514.
[5] Y. Zhou and W. Xue, "A multisensor fusion method for tool condition monitoring in milling," *Sensors*, vol. 18, no. 11, p. 3866, Nov. 2018.
[6] X. Lu, Z. Jia, X. Wang, Y. Liu, M. Liu, Y. Feng, and S. Y. Liang, "Measurement and prediction of vibration displacement in micro-milling of nickel-based superalloy," *Measurement*, vol. 145, pp. 254–263, Oct. 2019.
[7] N.-C. Tsai, D.-C. Chen, and R.-M. Lee, "Chatter prevention for milling process by acoustic signal feedback," *Int. J. Adv. Manuf. Technol.*, vol. 47, nos. 9–12, pp. 1013–1021, Apr. 2010.
[8] P. Huang, J. Li, J. Sun, and M. Ge, "Milling force vibration analysis in high-speed-milling titanium alloy using variable pitch angle mill," *Int. J. Adv. Manuf. Technol.*, vol. 58, nos. 1–4, pp. 153–160, Jan. 2012.
[9] M. M. E. F. Lamraoui, "Chatter detection in CNC milling processes based on Wiener-SVM approach and using only motor current signals," in *Vibration Engineering and Technology of Machinery*. Cham, Switzerland: Springer, Sep. 2014, pp. 567–578.
[10] Y. Du, Q. Song, Z. Liu, B. Wang, and Y. Wan, "Size-dependent responses of micro-end mill based on strain gradient elasticity theory," *Int. J. Adv. Manuf. Technol.*, vol. 100, nos. 5–8, pp. 1839–1854, Feb. 2019.
[11] M. L. Polli, W. L. Weingaertner, R. B. Schroeter, and J. D. O. Gomes, "Analysis of high-speed milling dynamic stability through sound pressure, machining force and tool displacement measurements," *Proc. Inst. Mech. Eng., B, J. Eng. Manuf.*, vol. 226, no. 11, pp. 1774–1783, Nov. 2012.
[12] Z. Wang, X. Liu, M. Li, S. Y. Liang, L. Wang, Y. Li, and B. Meng, "Intelligent monitoring and control technology of cutting chatter," *J. Mech. Eng.*, vol. 56, no. 24, pp. 1–23, 2020.
[13] H. Zhang, D. Anders, M. Löser, S. Ihlenfeldt, J. Czarske, and R. Kuschmierz, "Non-contact, bi-directional tool tip vibration measurement in CNC milling machines with a single optical sensor," *Mech. Syst. Signal Process.*, vol. 139, May 2020, Art. no. 106647.
[14] J. Binghui and F. Yong, "An optical fiber measurement system design on tool radial vibration," *Vibroeng. Procedia*, vol. 14, pp. 18–22, Oct. 2017.
[15] D.-C. Ye, "Turbine blade tip clearance measurement using a skewed dual-beam fiber optic sensor," *Opt. Eng.*, vol. 51, no. 8, May 2012, Art. no. 081514.
[16] B. Jia, L. He, G. Yan, and Y. Feng, "A differential reflective intensity optical fiber angular displacement sensor," *Sensors*, vol. 16, no. 9, p. 1508, Sep. 2016.
[17] I. García, J. Zubia, J. Beloki, J. Arrue, G. Durana, and G. Aldabaldetreku, "Optical tip clearance measurements as a tool for rotating disk characterization," *Sensors*, vol. 17, no. 12, p. 165, Jan. 2017.
[18] S. Maske, P. B. Buchade, and A. D. Shaligram, "A novel fiber bundle configuration for concurrent improvement of displacement range and sensitivity of self-referenced fiber optic displacement sensor," *Opt. Laser Technol.*, vol. 98, pp. 339–343, Jan. 2018.
[19] B. Jia, J. Yu, Y. Feng, M. Zhang, and G. Li, "Design of a reflective intensity optical fiber bundle displacement sensor," *J. Harbin Inst. Technol.*, vol. 27, no. 4, pp. 84–96, 2020.

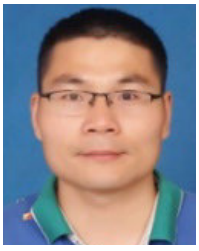

BINGHUI JIA was born in Heze, Shandong, China, in 1983. He received the B.S. degree in electronic information engineering from the Nanyang Institute of Technology, Henan, in 2008, and the M.S. and Ph.D. degrees in aerospace propulsion theory and engineering form Northwestern Polytechnical University, Xi'an, in 2013.

Since 2013, he has been a Lecturer and an Associate Professor with the School of Mechanical Engineering, Nanjing Institute of Technology, Nanjing. He is the author of more than 20 articles. His research interests include optical fiber sensor design and applications, micro-milling chatter measurement, and prediction and active control.

JING YU received the B.S. degree in mechanical engineering from the School of Mechanical Engineering, Nanjing Institute of Technology, Nanjing, China, in 2018. He is currently pursuing the M.S. degree in mechanical engineering with the Nanjing Institute of Technology.

His research interest includes the high-speed metal cutting processing and precision measurement of the tool vibration based on optical fiber sensor.